Protein Partitioning and Transport in Supported Cationic Acrylamide-Based Hydrogels

Shawn M. Russell, Emily B. Belcher, and Giorgio Carta
Dept. of Chemical Engineering, University of Virginia, Charlottesville, VA 22904

The partitioning and transport of myoglobin in cationic, acrylamide-based hydrogels are studied by a microscopic visualization method. Homogeneous cationic gels are synthesized inside fused-silica capillaries with a square section, which allow a direct determination of protein concentration profiles during transient adsorption and desorption. Diffuse, self-similar profiles are observed and used to determine the equilibrium protein binding capacity and the protein diffusivity in the gel. Mass-transfer rates are found to be essentially independent of the external solution concentration, but to vary dramatically with the gel polymer concentration. A Fickian diffusion model with a flux based on the adsorbed-phase concentration gradient is consistent with the experimentally determined concentration profiles for both positive and negative protein concentration steps. The equilibrium and rate parameters determined for the capillary-supported gels also compare favorably with those obtained from macroscopic measurements using composite ion-exchange media comprising similar gels held within the pores of porous silica particles.

Introduction

Charged gels are used extensively in adsorptive, ion-exchange chromatography separations (Boschetti, 1994). In addition, hydrogel-based materials find uses in biomedical applications for drug delivery, as components in diagnostic devices, and as physical models for in-vitro studies of partitioning and transport in tissue (Praveen, 1988; Conaghey et al., 1998; Prabhu et al., 1998).

Charged, freestanding hydrogels suitable for protein separations typically have only a limited mechanical strength (Kapur et al., 1996). Moreover, they can exhibit large volume changes in response to solution composition changes, especially at low cross-linking percentages (Baker et al., 1994). As a result, these materials can only be used in chromatography columns at low flow rates of the mobile phase. In recent years, however, composite chromatography particles obtained by incorporating a charged polyacrylamide gel in the pores of silica particles, as described by Girot and Boschetti (1993), have become commercially available with the trade name HyperD. Composite membranes have also been developed by incorporating these gels within the pores of filter media (Kapur et al., 1996). In these materials, the gel is stabilized against osmotic and mechanical forces by the rigid support matrix.

Partitioning and diffusion of proteins and other macromolecules in neutral gels has been investigated extensively both experimentally and theoretically (Ogston, 1958; Fawcett and Morris, 1966; Phillips et al., 1989; Park and Johnson, 1990; Boyer and Hsu, 1992; Amsdem, 1998). In these gels, the partition coefficient is less than one and the diffusivity is always less than in a free solution because of steric and hydrodynamic hindrance. In charged gels, however, partitioning of oppositely charged macromolecules can be very favorable (Sassi et al., 1996) and partition coefficients much greater than one can be achieved. In turn, while the diffusivity of macromolecules in these gels is certainly lower than in a free solution, transport rates can be greater than what could be obtained in a free solution because of the large diffusional driving force. Moreover, in these charged systems electrokinetic effects may be important contributing to increased or decreased mass-transfer fluxes (Probstein, 1989).

A number of macroscopic studies on protein adsorption on HyperD media have been conducted (Boschetti et al., 1995;

Correspondence concerning this article should be addressed to G. Carta.

Fernandez and Carta, 1996; Weaver and Carta, 1996; Rodrigues et al., 1995; Wright et al., 1998; Lewus and Carta, 1999). These particles have been shown to possess very high protein binding capacity and very high mass-transfer rates. Models accounting for a diffusive flux within the adsorbed-phase have been employed to describe mass transfer in these materials (Fernandez and Carta, 1996; Weaver and Carta, 1996; Wright et al., 1998). Similarly, models accounting for parallel pore and surface diffusion fluxes have been proposed to describe mass transfer in other ion exchangers (Yoshida et al., 1994; Blomingburg and Carta, 1994; Ma et al., 1996; Maekawa et al., 1998; Chen et al., 2002). Direct evidence for such a contribution to the mass-transfer flux is, however, difficult to obtain solely from macroscopic measurements of adsorption rates, since different rate models often yield qualitatively similar uptake curves (Linden et al., 2002). On the other hand, methods based on a visualization of intraparticle concentration profiles are generally considered to yield greater insight in this regard. Recently, confocal microscopy has been used to observe the evolution of concentration profiles of fluorescently labeled proteins in spherical ion exchange particles. The technique was originally introduced by Ljunglöf and Hjort (1996) and has recently been adapted to multicomponent systems (Linden et al., 1999, 2002).

A microscopic technique to visualize protein transport in charged gels synthesized within small capillaries has also been recently developed by Lewus and Carta (1999, 2001). Compared to measurements with spherical particles, the linear geometry of the capillaries provides several advantages. First, the quantitative interpretation of the images is simpler since fluorescence attenuation issues encountered when making measurements with spherical particles are avoided altogether. Secondly, in the linear geometry, the binding sites are uniformly distributed along the axial direction, while they are of course concentrated near the outer surface along the radial direction of the particle. Thirdly, since the gels are confined in a fixed control volume, the gel properties are known exactly. Finally, using gel-filled capillaries of sufficient length, the physical situation approximates a semi-infinite slab geometry, which allows a simple calculation of the diffusivity.

In previous work, Lewus and Carta (2001) have studied the partitioning and transport of cytochrome *c* (a positively charged protein at the experimental conditions) within an anionic acrylamide-based hydrogel. This protein was found to partition very favorably in the gel with an essentially rectangular isotherm. For certain conditions, the rate of mass transfer in the gel was very fast and essentially identical concentration profiles and mass-transfer rates were obtained, while varying the external protein concentration (Lewus and Carta, 2002). In this work, we extend the studies of Lewus and Carta to a cationic, acrylamide-based gel with a negatively charged protein. It is important to determine if the observations of Lewus and Carta can be extended to other systems, and if similar trends can be seen with regards to the effects of gel properties. Thus, the first objective of this study is to determine the mechanism of protein transport in the cationic gel by examining the evolution of protein concentration profiles under different conditions. The second objective is to observe the effects of changing the polymer concentration of the gel on the partitioning and mobility of the protein in the gel. A final objective is to compare rate measurements obtained with gel filled capillaries with macroscopic rate measurements obtained with gel-filled particles.

Materials and Experimental Methods

Preparation of gels

Optically clear, cationic gels were synthesized *in situ* within fused silica capillaries with a square section. Myoglobin from horse skeletal muscle (99% purity, $M_r = 17{,}600$, pI = 7.0) obtained from Sigma Chemical Co. (St. Louis, MO) was used as a model protein. This protein has an intense reddish-brown color, so that the evolution of concentration profiles in the gel can be directly viewed with a microscope. The cationic gels used in this work were prepared with a method analogous to that described by Lewus and Carta (1999) for the preparation of anionic gels using a water-soluble functionalized monomer, a cross-linker, an initiator, and a promoter. The functionalized monomer [3-methacryloylamino)propyl] trimethyl ammonium chloride (MAPTAC) was obtained from Aldrich Chemical Co. Inc. (Milwaukee, WI) as a 50 wt. % aqueous solution containing 600 ppm monomethyl ether hydroquinone inhibitor, which was removed with three activated carbon treatments. The crosslinker N,N′ methylene bis-acrylamide (MBA), the initiator ammonium persulfate (AP), and the promoter N,N,N′,N-tetramethyl ethylene diamine (TEMED) were obtained from Sigma Chemical Co. (St. Louis, MO). Fused silica, polyimide-coated square capillaries (100 μm I.D., 300 μm O.D.) were obtained from Polymicro Technologies (Phoenix, AZ). The capillaries were cut in 1-cm sections and the polyimide coating burned-off from the top 0.5 cm. The sections were then treated with bind-silane (γ-methacryloxy-propyl-trimethoxysilane) obtained from Amersham Pharmacia Biotech (Piscataway, NJ) to provide a way of anchoring the gel to the capillary wall by a covalent attachment.

For the preparation of a standard gel, a solution containing 0.2 g of MAPTAC, 0.01 g MBA, 0.01 g AP, and 1 μL TEMED per cm^3 was prepared with distilled, deionized, degassed water. The solution was then quickly injected into the capillaries, which were then placed in a helium box. After completion of the reaction (about 1 h), the gel-filled capillary sections were placed in a large volume of 50 mol/m^3, pH 9.6 Tris-HCl buffer containing 1 mol/m^3 sodium azide as a bacteriostatic agent for a minimum of 24 h.

The degree of incorporation of the monomer in the gel was determined by placing a precisely known volume of the polymerization mixture (4.0 cm^3) in a test tube. Following polymerization, the gel was carefully removed from the test tube and cut in small pieces, a few mm in size. These pieces were placed in a volume of distilled, deionized water for 48 h to remove any unreacted monomer from the gel. Following this, the gel fragments were recovered by filtering on filter paper and dried in a vacuum oven at 40°C. The degree of incorporation of the monomer was determined from the dry weight of the sample. The results gave >98% recovery of the initial monomer weight confirming that a nearly complete incorporation is obtained. Similar results have been reported by Gelfi and and Righetti (1981) for acrylamide-bisacrylamide gels. Assuming 100% incorporation, the standard gel used in this work has a polymer concentration of 0.21 g/cm^3, a cross-link density of 5% (w/w), and a charge density of 906 μmol/cm^3.

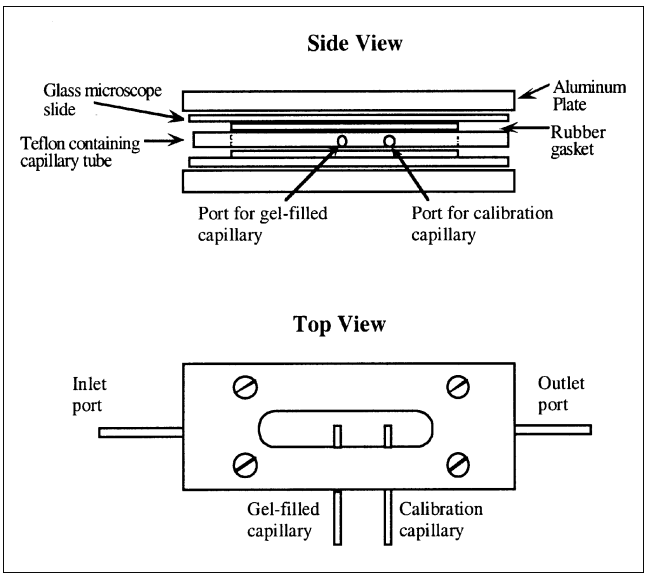

Figure 1. Flow cell for diffusion studies.

Gels with different polymer concentrations and charge density were prepared using different initial monomer concentrations, while maintaining the same ratio of monomer and cross-linker.

Measurement of concentration profiles

The flow cell and the microscope setup are given in Figures 1 and 2. The cell consists of a 1/8-in. thick Teflon slab sandwiched between two microscope slides with thin silicon gaskets held together by two aluminum plates. The gel-filled capillary sections were clipped by scoring the surface with a ceramic blade, which resulted in a fairly sharp interface. The uncut end was then glued to the tip of syringe needles (21 gage) using a cyanoacrylate adhesive, and inserted in the cell through a hole bored on the side of the Teflon slab. Since the polymer is attached to the inner capillary wall through the bind-silane chemistry, the gel volume remained constant during the experiments making it possible to determine accurately the position of the gel-solution interface. A second hole in the Teflon slab was used to insert calibration capillaries identical to those containing gel, but filled with protein solutions with known concentration and sealed. Inlet and outlet ports bored into the short sides of the Teflon slab were used to flow the protein solution transversely across the tip of the gel-filled capillary.

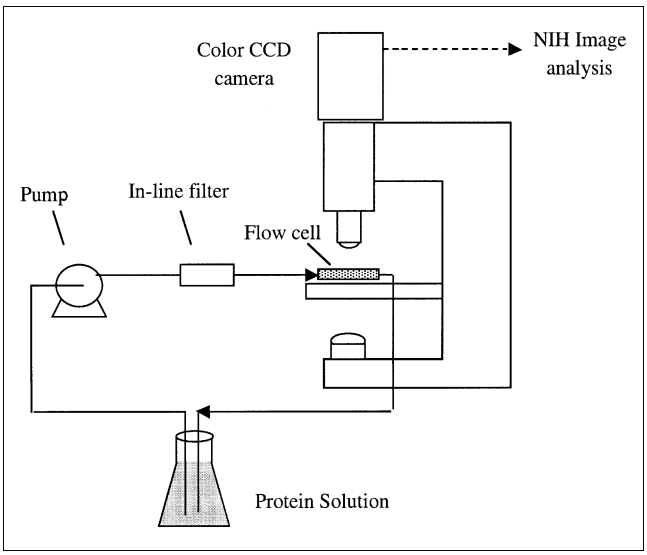

Figure 2. Apparatus for diffusion studies.

The protein solution was fed to the flow cell with a Cole-Parmer (Chicago, IL) peristaltic pump at 0.7 cm^3/min, which corresponds to a linear velocity past the tip of the capillary of 185 cm/h. A Nikon Eclipse E200 microscope at 100× magnification was used to observe the evolution of concentration profiles in the gel. Digital images were collected using a Sanyo Hi-Resolution Color CCD camera interfaced to a Power Mac 7100/80 computer. The program NIH Image (a public domain program developed at the U.S. National Institute of Health and available on the Internet at http://rsb.info.nih.gov/nih-image/) was used to obtain the grayscale values of the digitized images. These values were converted to adsorbed protein concentrations based on a calibration curve using grayscale values measured for the calibration capillaries. This curve was obtained by plotting the grayscale values GS vs. the protein concentration C in the form suggested by the Lambert-Beer law as

$$-\ln\left(1-\frac{GS}{\gamma}\right)=\beta C \tag{1}$$

The values $\gamma = 183$ and $\beta = 0.0059$ cm^3/mg yielded a straight line with a correlation coefficient of 0.992 over the range $C = 0$–340 mg/cm^3.

All experiments were performed at room temperature (21 ±2°C) in 50 mol/m^3 Tris-HCl buffer at pH 9.6. At this pH (2.6 units higher than the protein pI), myoglobin has a strong negative charge.

Macroscopic measurements

The equilibrium and rate of myoglobin binding were also determined for gel-filled particles. Q-HyperD-M particles, obtained from BioSepra, Inc. (Marlborough, MA), were used in these experiments. These particles consist of a cationic acrylamide-based gel similar to the standard gel described above contained within the pores of a silica support matrix (Girot and Boschetti, 1993; Fernandez and Carta, 1996). The sample used in this work had an average particle diameter of 76 μm, and the standard deviation of the particle-size distribution was 17 μm. The porosity of the support matrix is around 0.6. Equilibrium isotherms were obtained by a batch equilibrium method and adsorption rates were determined in a stirred vessel apparatus as described by Fernandez and Carta (1996).

Results

Equilibrium binding capacity

The equilibrium binding capacity for myoglobin was obtained by placing gel-filled capillaries in myoglobin solutions of known concentrations for 100 h. The gels were then removed from solution and placed in the flow cell to determine

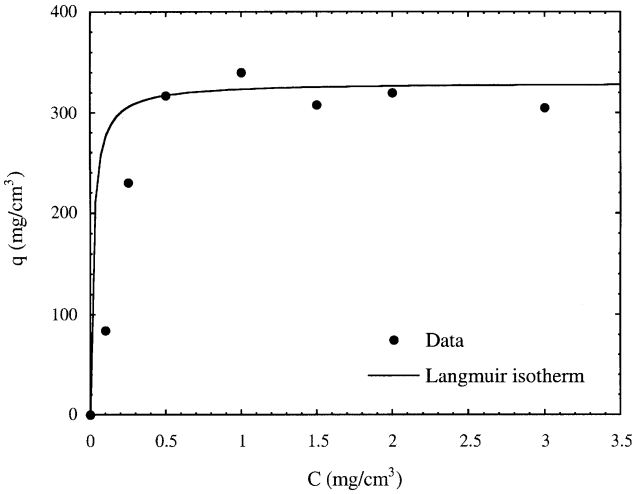

Figure 3. Adsorption isotherm for myoglobin on capillary supported gel.

Polymer concentration = 0.21 g/cm^3.

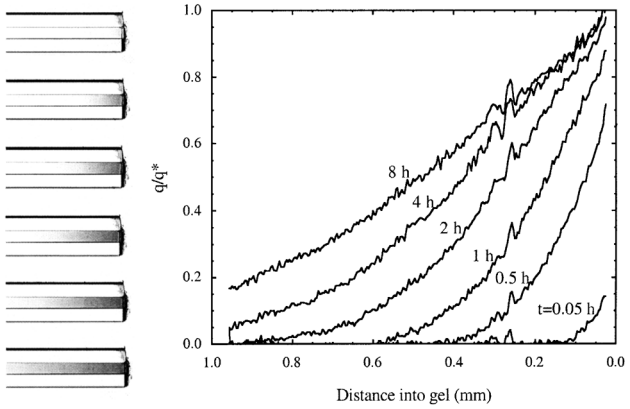

Figure 4. Transient adsorption of myoglobin in capillary supported gel.

Protein concentration = 1 mg/cm^3; polymer concentration = 0.21 g/cm^3. Images and concentration profiles are shown at 0.05, 0.5, 1, 2, 4, and 8 h.

the protein concentration in the saturated gel from the grayscale values. The results are given in Figure 3. It is evident that the equilibrium binding of myoglobin is very favorable with a maximum capacity of 340 ± 30 mg/cm^3. The Langmuir isotherm given by

$$q = \frac{q_m b C}{1 + bC} \tag{2}$$

was used to fit the equilibrium data with $q_m = 340$ mg/cm^3 and $b = 50$ cm^3/mg and the calculated line is shown in Figure 3. A similarly favorable isotherm and a similar capacity was observed by Lewus and Carta (2001) for cytochrome c ($M_r \sim$ 12,500) on an analogous anionic gel with the same polymer concentration and cross-linking. Assuming a value of 0.7 cm^3/mg for the specific volume of the protein (Mahler and Cordes, 1966), the maximum capacity observed for myoglobin corresponds to a protein volume fraction in the gel of 0.24 ± 0.02. This high value suggests that protein binding occurs through a three-dimensional (3-D) filling of the gel. Very high binding capacities for proteins have also been previously reported for Q-HyperD media. For example, a capacity of 220 mg/cm^3 has been obtained for BSA ($M_r \sim 65{,}000$) on Q-HyperD-M by Fernandez and Carta (1996).

Transient adsorption and desorption experiments

The evolution of myoglobin concentration profiles during transient adsorption in the standard gel from 1 mg/cm^3 protein solution is shown in Figure 4. The images on the left show the myoglobin band advancing through the gel from right to left. Approximately 1 mm of capillary is visible in these images and the lightly colored area surrounding the capillary corresponds to the dilute protein solution circulated through the cell in the experiment. The graph on the right shows the digitized concentration profiles normalized with respect to the saturation capacity q^* at times corresponding to the images on the left. Due to imperfections in the way the capillaries were cut and the resulting optical artifacts, it was not possible to accurately determine the profiles very near the exposed end of the capillary. However, it is evident from this figure that myoglobin diffuses gradually through the gel forming smooth concentration profiles. This result is extremely important and suggests that the protein retains diffusional mobility in the gel. In fact, if myoglobin were not mobile in the gel, given the sharpness of the binding isotherm, one would expect to see a sharp advancing front (Lewus and Carta, 2002). Clearly, this is not seen experimentally. Lewus and Carta (2001) have obtained a similar result for cytochrome c in the analogous anionic gel, suggesting that transport mechanisms in the two different systems are similar.

The effect of the protein concentration in solution on the concentration profiles in the gel is shown in Figure 5 for experiments with 1 and 2 mg/cm^3 myoglobin solutions. As seen in Figure 3, both of these concentrations are in the flat portion of the isotherm; hence, q^* is essentially the same in both cases. Remarkably, as seen in Figure 5, the profiles obtained at the two different concentrations are also essentially coincident. As a result, it can be inferred that the driving force for transport of myoglobin in the cationic gel is dependent on the adsorbed-phase concentration, not on the liquid-phase concentration. Since the adsorbed-phase concentration is practically invariant, the rate of mass transfer is essentially the same in the two experiments.

Figure 6 shows the results of an experiment where the standard gel was exposed to a 1 mg/cm^3 solution of myoglobin for 2 h. After this 2 h period, the myoglobin solution was flushed out of the cell and replaced with 50 mol/m^3 Tris-HCl buffer. The top figure shows the digitized concentration profiles from the 2 h mark on, while the bottom figure shows the total amount of protein in the gel as a function of time obtained by integrating the concentration profile. Approximately 0.9 μg of myoglobin are adsorbed during the first 2 h. After placing the gel in buffer, while very little protein is desorbed, the protein concentration profiles continue to evolve. It is evident that the protein retains mobility within the gel and continues to diffuse largely from right to left even after

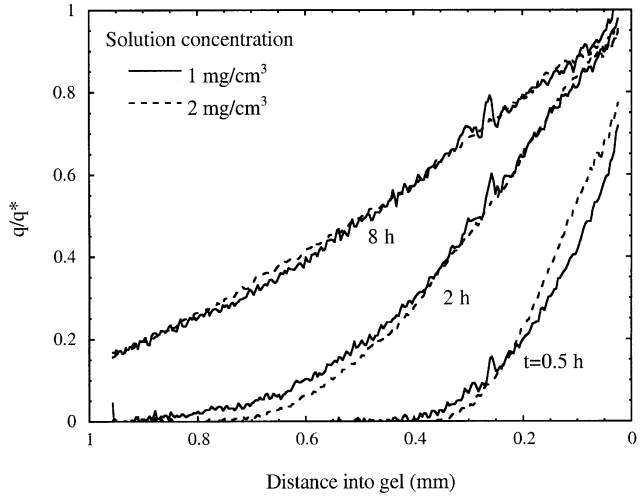

Figure 5. Effect of protein concentration in solution on transient adsorption of myoglobin in capillary supported gel.

Protein concentrations = 1 and 2 mg/cm^3; polymer concentration = 0.21 g/cm^3. Concentration profiles are shown at 0.5, 2, and 8 h.

the protein is removed from solution. At the same time, little protein is desorbed from the gel. This occurs because the binding isotherm is very favorable, and the external boundary layer mass-transfer resistance becomes limiting as a result of the very small concentration driving force in the liquid phase.

Desorption of myoglobin from the gel with salt is shown in Figure 7. In this experiment the gel was first exposed to a 1 mg/cm^3 solution of myoglobin in 50 mol/m^3 Tris-HCl buffer for 4 h and then to 50 mol/m^3 Tris-HCl buffer containing 500 mol/m^3 NaCl. In this case, the concentration of myoglobin at the gel-solution interface rapidly approaches zero and the protein diffuses quickly out of the exposed end of the capillary. After 2 h, nearly all of the myoglobin has been removed from the gel. In this case, the high salt concentration shields the favorable electrostatic interaction between the negatively charged protein and the positively charged functional groups in the gel, allowing rapid diffusion of the protein. Since, for these conditions, there is no protein binding at the gel-liquid interface, the external boundary layer resistance is insignificant.

Figure 8 shows the effect of the gel polymer concentration on the concentration profiles obtained after 4 h of exposure to a 1 mg/cm^3 myoglobin solution. The charge density also varied in proportion to polymer concentration for the different gels, although the cross-link density was kept constant at 5%. At a low polymer concentration, the charge density is lower, which can be expected to reduce the binding capacity. However, the diffusional hindrance can also be expected to be lower, which should result in faster diffusion. Conversely, at a high gel polymer concentration, the charge density is higher, but the gel mesh is tighter, resulting in a greater diffusional hindrance. These trends are clearly seen in Figure 8. The greatest depth of penetration is attained with the 0.16 g/cm^3 gel. The maximum equilibrium binding capacity occurs with the 0.32 mg/cm^3 gel. However, the greatest amount of protein adsorbed in 4 h is obtained with the 0.21 g/cm^3 gel.

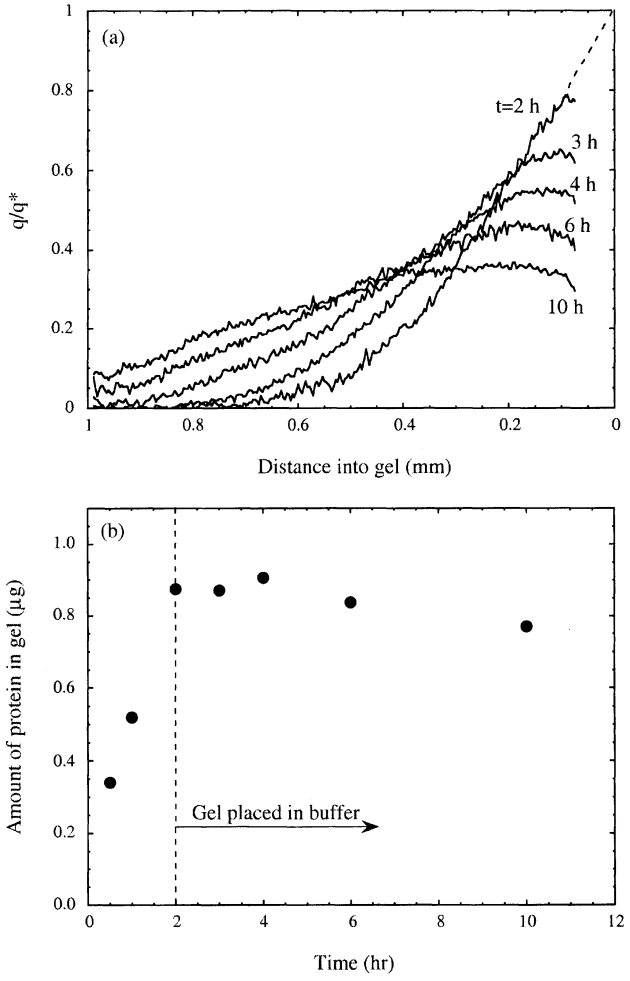

Figure 6. Effect of exposing a capillary-supported gel to buffer following exposure to protein.

Protein concentrations = 1 mg/cm^3 for 2 h, then 0; polymer concentration = 0.21 g/cm^3. (a) Concentration profiles shown at 2, 3, 4, 6, and 10 h. (b) Amount of protein in gel as a function of time.

More concentrated gels result in much lower adsorption rates likely because of steric effects.

Quantitative analysis

The quantitative analysis follows the approach of Lewus and Carta (2001) and is based on the following Fickian diffusion model

$$\frac{\partial q}{\partial t} = \frac{\partial}{\partial z}\left[D_s(q)\frac{\partial q}{\partial z}\right] \tag{3}$$

$$t = 0: \qquad q = 0 \tag{3a}$$

$$z = 0: \quad -D_s(q)\frac{\partial q}{\partial z} = k_f(C - C_s) \tag{3b}$$

$$z \to \infty: \quad \frac{\partial q}{\partial z} = 0 \tag{3c}$$

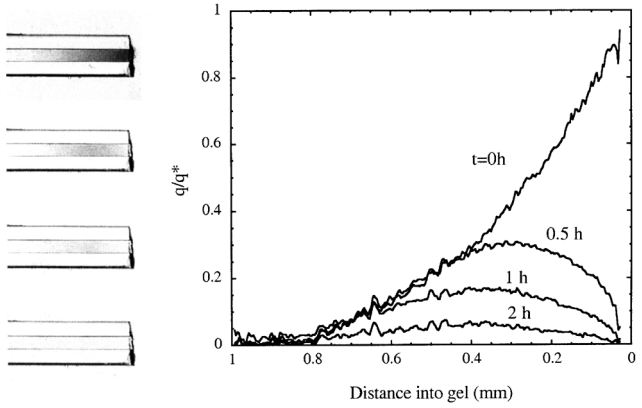

Figure 7. Desorption of myoglobin from capillary-supported gel by exposure to 500 mol/m^3 NaCl in 50 mol/m^3 Tris-HCl buffer at pH 9.6 following adsorption from 1 mg/cm^3 myoglobin for 4 h.

Polymer concentration = 0.21 g/cm^3. Images and concentration profiles are shown at 0, 0.5, 1, and 2 h from the beginning of exposure to 500 mol/m^3 NaCl.

where $D_s(q)$ is a concentration-dependent diffusion coefficient and k_f is the external boundary layer mass-transfer coefficient. Lewus and Carta (2001) have determined a value of $k_f = 2\times10^{-3}$ cm/s for cytochrome *c* in the same cell with a linear fluid velocity of 120 cm/h. The k_f value for myoglobin under the experimental conditions of this work was estimated to be 2.5×10^{-3} cm/s assuming a square-root dependence on fluid velocity and a 2/3-power dependence on the solution diffusivity, based on well established mass-transfer correlations (Cussler, 1997). As shown later, for these conditions, the boundary layer resistance is negligible for adsorption from a 1 mg/cm^3 myoglobin solution, except for very short times. If these are neglected, boundary condition 3b is replaced with

$$z = 0: \quad q = q^* \tag{3d}$$

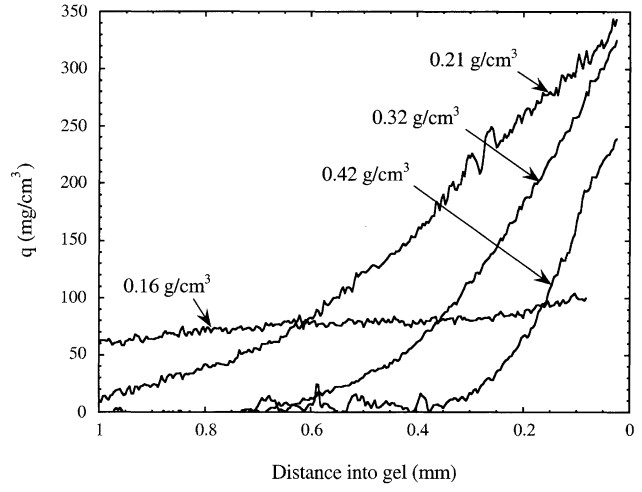

Figure 8. Effect of polymer gel on transient adsorption of myoglobin in capillary supported gel.

Protein concentration = 1 mg/cm^3. Concentration profiles are shown at 4 h of exposure.

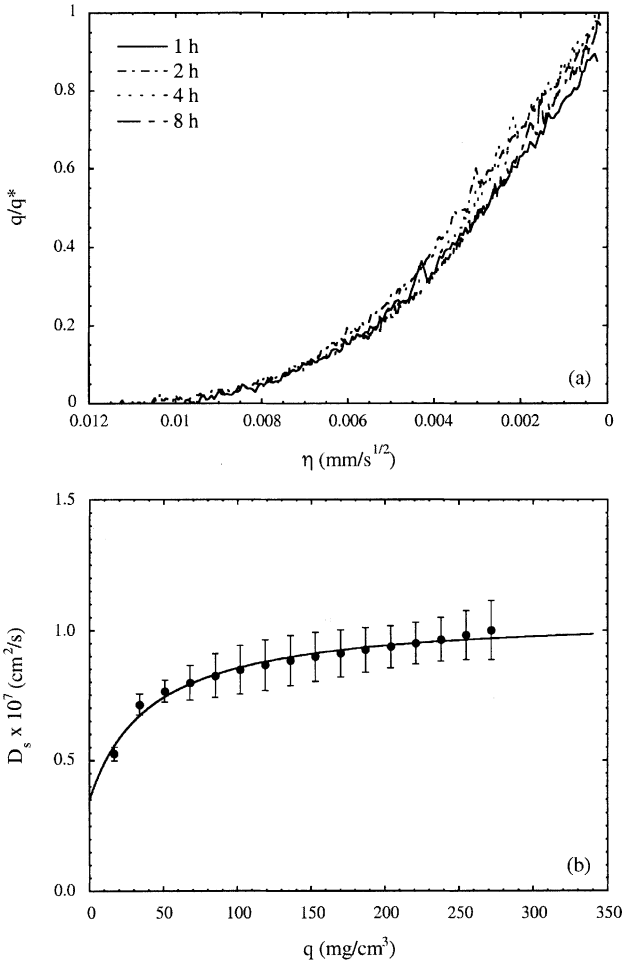

Figure 9. (a) Concentration profiles of Figure 4 plotted as a function of η; (b) calculated diffusivity D_s.

Error bars in (b) are based on calculated values of D_s at 1, 2, and 4 h.

In this case, by applying the Boltzmann transformation

$$\eta = \frac{z}{\sqrt{t}} \tag{4}$$

the concentration profiles can be shown to be self-similar. That is, they should coincide when plotted vs. η. A plot for the data of Figure 4 vs. η is shown in Figure 9a. It can be seen that the profiles at 1, 2, 4, and 8 h collapse closely onto a single line, confirming that the experimental behavior is consistent with Fick's law. In this case, the diffusivity can be obtained from

$$D_s(q) = -\frac{\int_0^q \eta dq}{2\left(\frac{dq}{d\eta}\right)} \tag{5}$$

Calculated diffusivities are shown in Figure 9b. As seen in this figure, the D_s-values are contained within a factor of

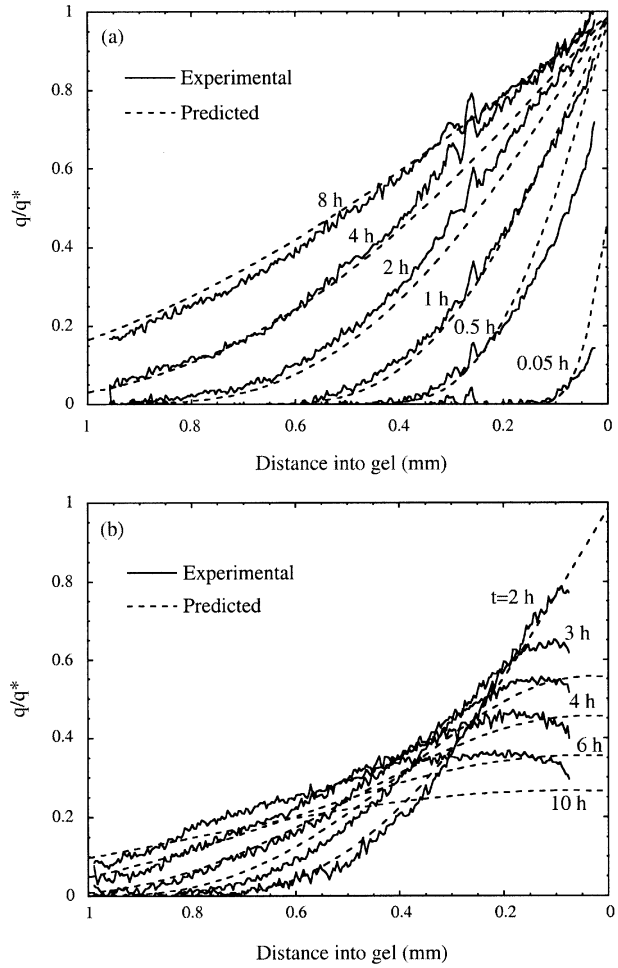

Figure 10. Comparison of experimental and predicted concentration profiles.

(a) Myoglobin adsorption; (b) myoglobin desorption in buffer. Conditions in Figures 4 and 6.

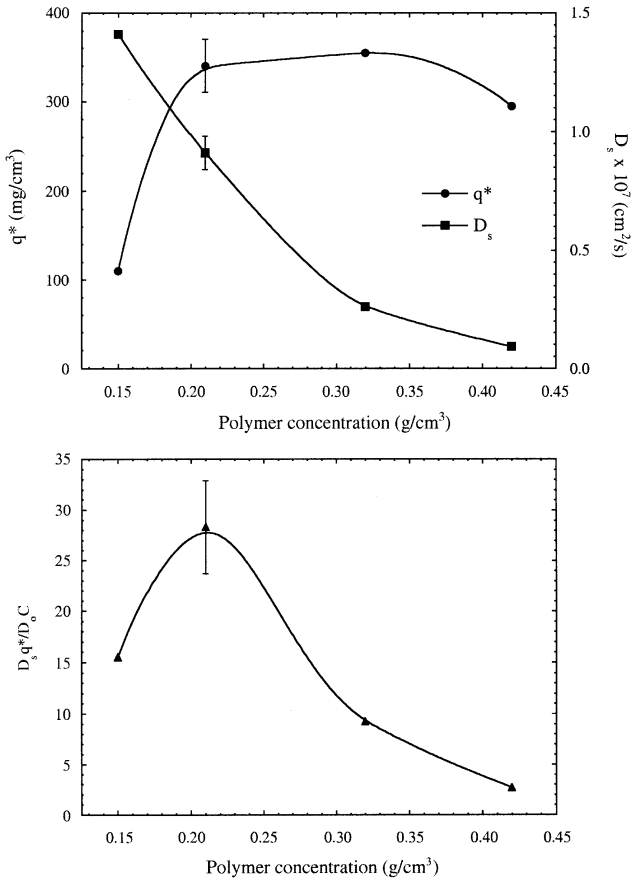

Figure 11. Effect of polymer gel concentration on (a) diffusivity and adsorption capacity and (b) ratio $D_s q^*/D_0 C$.

about 2 and become nearly independent of q when q exceeds 100 mg/cm^3. Lewus and Carta (2001) also observed this behavior for cytochrome *c* in the analogous anionic gel. However, the diffusivity of myoglobin is about three times higher than that of cytochrome *c*, in spite of the fact that the molecular mass of myoglobin is larger than that of cytochrome *c* and that these two proteins have essentially the same solution diffusivity (Tyn and Gusek, 1990). It is likely that other factors, including the different net charge of the two proteins, the different distribution of charges on the protein, and their different shapes, contribute to the difference in diffusivities in the charged gels.

Figure 10 compares experimental and predicted concentration profiles for the experiments shown in Figures 4 and 6. The predicted profiles are based on Eq. 3 with boundary conditions 3a–3c using the isotherm in Figure 3, a value of $k_f = 2.5\times10^{-3}$ cm/s, and the empirical $D_s(q)$ relationship shown in Figure 9b. The solution was obtained by finite differences. There is obviously a very good agreement between experimental and predicted profiles in Figure 10a. This can be expected, since the diffusivity was obtained from the same data. However, the model predictions confirm that the external boundary layer resistance is indeed minimal for these conditions except for very early times. Moreover, model predictions are also in reasonable agreement with the desorption profiles in Figure 10b. The model slightly overpredicts the desorption rate, although it captures the qualitative trends quite well. A certain amount of irreversible binding of myoglobin on the gel was noted after very long times, and it is likely that this contributed to the difference between predicted and experimental profiles near the exposed portion of the gel.

The predicted effect of solution concentration was also found to be in excellent agreement with the experimental results. Since the isotherm is very favorable and the driving force for diffusion is given by the gradient $\partial q/\partial z$, the model predicts identical concentration profiles at 1 and 2 mg/cm^3, which is in good agreement with the experimental observations in Figure 5.

The same quantitative analysis was also used to determine the myoglobin diffusivity in gels with different polymer concentration and charge density. The results are given in Figure 11. For simplicity, only the values of q^* and the values of D_s extrapolated to $q = q^*$ are shown. The values of the ratio $D_s q^*/D_0 C$, where $D_0 = 1.1\times10^{-6}$ cm^2/s is the liquid-phase diffusivity of myoglobin (Tyn and Gusek, 1990), are also of

interest and are shown in Figure 11b. This ratio is representative of the ratio of the actual rate of mass transfer, and the rate of mass transfer that would be seen if diffusion occurred in the liquid phase with a liquid-phase concentration driving force (Lewus and Carta, 2001, 2002). As seen in this graph, the rate of mass transfer in these gels is higher than it would be in solution. This happens because of the high binding capacity of the gel coupled with a fairly high diffusivity D_s. It is apparent that, as the gel polymer concentration is increased, the rate becomes substantially smaller because of the sharp drop in diffusivity. Conversely, as the gel polymer concentration is reduced to low values, the rate becomes smaller because of the sharp drop in adsorption capacity. As previously noted, the highest mass-transfer rates are obtained at an intermediate polymer concentration.

A final consideration to be made here is whether the diffusivities determined in this work could be predicted using established hydrodynamic hindrance models for macromolecules in fibrous gels. Tong and Anderson (1996), for example, showed that the diffusion coefficient of proteins in neutral polyacrylamide gels are predicted by the following equation

$$\frac{D_{\text{gel}}}{D_0} = \frac{1}{1+\sqrt{\frac{r_m^2}{k}}+\frac{1}{3}\frac{r_m^2}{k}} \tag{6}$$

where r_m is the radius of the diffusing molecule and k is the hydraulic permeability of the gel. The latter can be predicted from various correlations as discussed by Tong and Anderson, although the uncertainty is probably large. On the other hand, Kapur et al. (1996) have measured the hydraulic permeability of a membrane-supported positively charged polyacrylamide gel similar to the ones used in our work. Their gel had a polymer concentration of 0.17 g/cm^3 and a permeability $k = 0.420 \pm 0.035 \times 10^{-14}$ cm^2 at ionic strengths similar to that used in our work. Using this value of k for the gel and $r_m = 2.0$ nm for myoglobin, Eq. 6 yields $D_{\text{gel}} = 1.52 \pm 0.09 \times 10^{-7}$ cm^2/s. Comparing this value with the data in Figure 11a for gels with a similar polymer concentration, it appears that our experimental diffusivities are 20–30% lower than the value predicted by Eq. 6. Although differences between the gel used by Kapur et al. and those used in this work cannot be ruled out as the cause of this difference (their gel had a lower charge density than those used in our work), it is possible that the difference actually reflects an increased diffusional hindrance caused by the attractive electrostatic interaction between the negatively charged protein and the positively charged gel.

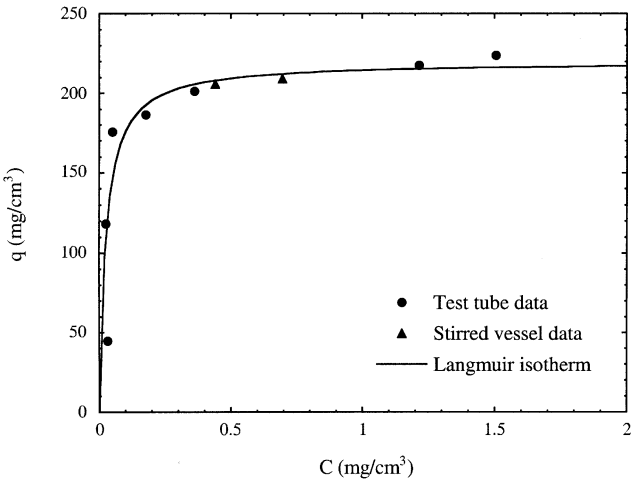

Figure 12. Adsorption isotherm for myoglobin on Q-HyperD-M in 50 mol/m^3 Tris-HCl buffer at pH 9.6.

The basis for q is the total particle volume. Stirred vessel data are from Figure 13 at $t = 1{,}700$ s.

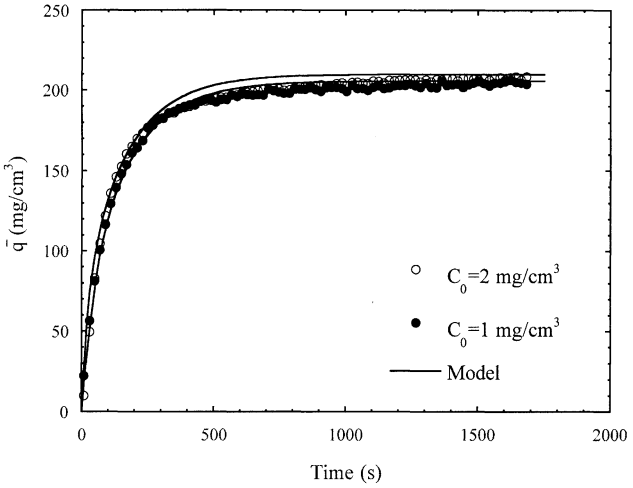

Figure 13. Batch uptake curves for myoglobin adsorption on Q-HyperD-M at 1.2 and 2.0 mg/cm^3 initial protein concentrations.

$V_M = 0.36$ and 0.61 cm^3 for the 1.2 and the 2.0 mg/cm^3 experiments respectively. $V = 100$ cm^3. The basis for $\bar{q}$ is the total particle volume.

Comparison with adsorption in gel-composite particles

Figure 12 shows the adsorption isotherm for myoglobin on Q-HyperD-M in 50 mol/m^3 Tris-HCl buffer at pH 9.6. The solid line shows the Langmuir isotherm fit with $q_m = 220$ mg/cm^3 and $b = 40$ cm^3/mg. The isotherm shape is similar to that obtained with the capillary supported gel. Figure 13 gives the results of two batch uptake experiments with initial myoglobin concentrations of 1 and 2 mg/cm^3 showing the average protein concentration in the particles $\bar{q}$ as a function of time. As seen in this graph, the two uptake curves are nearly coincident, a result consistent with the observations for the capillary supported gels. The solid lines in this graph represent model simulations based on Eq. 2 with the following conservation equations and boundary conditions

$$\frac{\partial q}{\partial t} = \frac{1}{r^2}\frac{\partial}{\partial r}\left[D_s(q) r^2 \frac{\partial q}{\partial r}\right] \tag{7}$$

$$t = 0: \quad q = 0 \tag{7a}$$

$$r = 0: \quad \frac{\partial q}{\partial r} = 0 \tag{7b}$$

$$r = r_p: \quad D_s(q)\frac{\partial q}{\partial r} = k_f(C - C_s) \tag{7c}$$

$$\frac{dC}{dt} = -\frac{V_M}{V}\frac{d\bar{q}}{dt} = -\frac{3k_f}{r_p}\frac{V_M}{V}(C - C_s) \tag{8}$$

$$t = 0: \quad C = C_0 \tag{8a}$$

which are analogous to those used to describe transport in the capillary supported gels. In these equations V_M is the volume of particles, V is the solution volume, r_p is the particle radius, and C_0 is the initial protein concentration in solution. For these calculations, we used a value of $k_f = 2\times10^{-3}$ cm/s, based on the results of Fernandez and Carta (1996), and a value of $D_s = 0.9\times10^{-8}$ cm^2/s obtained by fitting the batch uptake curves. As seen in Figure 13, a single value of D_s provides a very reasonable fit of both batch uptake curves.

Since, according to the patent literature (Girot and Boschetti, 1993), the composition of the HyperD gel is similar to that of the gels synthesized in this work, it should be possible to compare the binding capacity and diffusivity of myoglobin obtained for Q-HyperD-M with the data obtained for the capillary supported gels. To make this comparison, however, the porosity and tortuosity of the support matrix of Q-HyperD-M must be taken into account since protein binding and transport occur only within the gel-filling of the pores. Based on the support porosity $\epsilon_p \sim 0.6$ and an assumed tortuosity factor τ_p in the range 2 to 4, we obtain a corrected capacity value of 370 mg/cm^3 on a "per gel volume basis" and a corrected diffusivity in the range $0.7-1.2\times10^{-7}$ cm^2/s. These corrected values are quite consistent with the experimental values of q_m and D_s determined for the capillary supported gels. Recognizing that a perfect agreement cannot be expected since the exact composition of the Q-HyperD gel is not known, the substantial agreement obtained among these rather different determinations is remarkable.

Conclusions

Our study of the adsorption and diffusion of a negatively charged protein in a cationic acrylamide-based gel supported in silica capillaries shows that adsorption is very favorable and occurs quite rapidly. The evolution of protein concentration profiles in the gel and their response to the external conditions are consistent with a Fickian diffusion model where the driving force is expressed in terms of the adsorbed-phase concentration gradient. As a result, mass-transfer rates are essentially independent of the liquid-phase protein concentration when experiments are carried out in the flat portion of the isotherm. The polymer gel concentration has a large influence on the adsorption capacity and diffusion rate in the gel. Over the range of polymer concentrations studied, a one-order magnitude decline in the diffusion coefficient is observed as the polymer concentration is increased from 0.16 to 0.42 g/cm^3. The adsorption capacity, however, exhibits a maximum at 0.32 g/cm^3. The coupling of high adsorption capacity and diffusivity produce mass-transfer rates that are larger than what could be observed if diffusion occurred in free solution. The results obtained with capillary supported gels are both qualitatively and quantitatively consistent with those obtained from macroscopic measurements with gel-composite particles. A final consideration regards the ability of other rate models to describe these data. It can be surmised that an ordinary pore diffusion-adsorption model, where the mass-transfer flux is proportional to the fluid phase concentration gradient could also model the shape of the batch uptake curves at each concentration. However, as shown by the theoretical calculations of Lewus and Carta (2002), such a model could not describe the smooth profiles observed in the capillary experiments and the concentration-independent transient adsorption behavior obtained in the flat portion of the isotherm.

Acknowledgment

This research was supported by NSF Grant CTS-0079334.

Notation

b = Langmuir isotherm parameter, cm^3/mg
C = solution concentration, mg/cm^3
C_0 = initial solution concentration, mg/cm^3
C_s = solution concentration at gel-liquid interface, mg/cm^3
D_0 = free solution diffusion coefficient, cm^2/s
D_s = diffusion coefficient based on adsorbed-phase driving force, cm^2/s
k = hydraulic permeability, cm^2
k_f = boundary layer mass transfer coefficient, cm/s
M_r = molecular mass
q = adsorbed phase concentration, mg/cm^3
q_m = Langmuir isotherm parameter, mg/cm^3
q^* = equilibrium adsorbed-phase concentration, mg/cm^3
r = particle radial coordinate, cm
r_m = solute radius, cm
r_p = particle radius, cm
t = time, s
V = solution volume, cm^3
V_M = volume of particles, cm^3
z = distance into gel, cm
ϵ_p = support matrix void fraction
η = Boltzmann transformation variable ($z/\sqrt{t}$), cm/s$^{1/2}$
τ_p = support matrix tortuosity factor

Literature Cited

Amsden, B., "Solute Diffusion within Hydrogels. Mechanisms and Models," *Macromolecules*, **31**, 8382 (1998).

Baker, J. P., L. H. Long, H. W. Blanch, and J. M. Prausnitz, "Effect of Initial Total Monomer Concentration on the Swelling Behavior of Cationic Acrylamide-Based Hydrogel," *Macromolecules*, **27**, 1446 (1994).

Bloomingburg, G. F., and G. Carta, "Separation of Protein Mixtures by Continuous Annular Chromatography with Step Elution," *Chem. Eng. J.,* **55**, B19 (1994).

Boschetti, E., "Advanced Sorbents for Preparative Protein Separation Purposes," *J. Chromatog. A*, **658**, 207 (1994).

Boschetti, E., L. Guerrier, P. Girot, and J. Horvath, "Preparative High-Performance Liquid Chromatographic Separation of Proteins with HyperD Ion-Exchange Supports," *J. Chromatog. B*, **664**, 225 (1995).

Boyer, P. M., and J. T. Hsu, "Experimental Studies of Restricted Protein Diffusion in an Agarose Matrix," *AIChE J*., **38**, 259 (1992).

Chen, W.-D., X.-Y. Dong, and Y. Sun, "Analysis of Diffusion Models for Protein Adsorption to Porous Anion-Exchange Adsorbent," *J. Chromatog. A*, **962**, 29 (2002).

Conaghey, O. M., J. Corish, and O. I. Corrigan, "Iontophoretically Assisted in Vitro Membrane Transport of Nicotine from a Hydrogel Containing Ion Exchange Resins," *Int. J. Pharmaceutics*, **170**, 225 (1998).

Cussler, E. L., *Diffusion—Mass Transfer in Liquid Systems*, Cambridge University Press, 2nd ed., Cambridge, U.K., pp. 224–228 (1997).

Fawcett, J. S., and C. J. O. R. Morris, "Molecular-Sieve Chromatography of Proteins on Granulated Polyacrylamide Gels," *Sep. Sci.*, **1**, 9 (1966).
Fernandez, M. A., and G. Carta, "Characterization of Protein Adsorption by Composite Silica-Polyacrylamide Gel Anion Exchangers: I. Equilibrium and Mass Transfer in Agitated Contactors," *J. Chromatog. A*, **746**, 169 (1996).
Gelfi, C., and P. G. Righetti, "Polymerization Kinetics of Polyacrylamide Gels—I. Effect of Different Cross-Linkers," *Electrophoresis*, **2**, 213 (1981).
Girot, P., and E. Boschetti, "Passivated and Stabilized Porous Mineral Oxide Supports and Method for the Preparation and Use of the Same," U.S. Patent No. 5,268,097 (1993).
Kapur, V., J. Charkoudian, and J. L. Anderson, "Transport of Proteins through Gel-Filled Porous Membranes," *J. Memb. Sci.*, **131**, 143 (1997).
Kapur, V., J. C. Charkoudian, S. B. Kessler, and J. L. Anderson, "Hydrodynamic Permeability of Hydrogels Stabilized within Porous Membranes," *Ind. Eng. Chem. Res.*, **35**, 3179 (1996).
Lewus, R. K., and G. Carta, "Protein Diffusion in Charged Polyacrylamide Gels: Visualization and Analysis," *J. Chromatog. A*, **865**, 155 (1999).
Lewus, R. K., and G. Carta, "Binary Protein Adsorption on Gel-Composite Ion-Exchange Media," *AIChE J.,* **45**, 512 (1999).
Lewus, R. K., and G. Carta, "Protein Adsorption and Transport in Charged Gels and Chromatography Media for Protein Separations," *Fundamentals of Adsorption 7*, K. Kaneko, H. Kanoh, and Y. Hanzawa, eds., International Adsorption Society, IK International, Chiba, Japan, p. 117 (2002).
Lewus, R. K., and G. Carta, "Protein Transport in Constrained Anionic Hydrogels: Diffusion and Boundary Layer Mass Transfer," *Ind. Eng. Chem. Res.*, **40**, 1548 (2001).
Linden, T., A. Ljunglöf, L. Hagel, M.-R. Kula, and J. Thommes, "Visualizing Patterns of Protein Uptake to Porous Media using Confocal Scanning Laser Microscopy," *Sep. Sci. Techol*., **37**, 1 (2002).
Linden, T., A. Ljunglöf, M.-R. Kula, and J. Thommes, "Visualizing Two Component Protein Diffusion in Porous Adsorbents by Confocal Scanning Laser Microscopy," *Biotechnol. Bioeng.*, **65**, 622 (1999).
Ljuglöf, A., and R. Hjort, "Confocal Microscopy as a Tool for Studying Protein Adsorption to Chromatography Matrices," *J. Chromatog. A*, **743**, 75 (1996).
Ma, Z., R. D. Whitley, and N.-H. L. Wang, "Pore and Surface Diffusion in Multicomponent Adsorption and Liquid Chromatography Systems," *AIChE J.,* **42**, 1244 (1996).
Mahler, H. R., and E. H. Cordes, *Biological Chemistry*, Harper and Row, New York (1966).
Maekawa, M., K. Kasai, and M. Nango, "Transport Phenomena of Sulfonated Dyes into Cellulose Membranes: Parallel Diffusion of a Sulfonated Dye with a High Affinity onto Cellulose," *Colloids Surf. A*, **132**, 173 (1998).
Ogston, A. G., "The Spaces in a Uniform Random Suspension of Fibres," *Trans*. *Faraday Soc*., **54**, 1754 (1958).
Park, I. H., and C. S. Johnson, "Probe Diffusion in Polyacrylamide Gels as Observed by Means of Holographic Relaxation Methods: Search for a Universal Equation," *Macromolecules*, **23**, 1548 (1990).
Phillips, R. J., W. M. Deen, and J. F. Brady, "Hindered Transport of Spherical Macromolecules in Fibrous Membranes and Gels," *AIChE J.*, **35**, 1761 (1989).
Prabhu, S. S., W. C. Broaddus, G. T. Gillies, W. G. Loudon, Z. J. Chen, and B. Smith, "Distribution of Macromolecular Dyes in Brain using Positive Pressure Infusion: A Model for Direct Controlled Delivery of Therapeutic Agents," *Surg. Neurol.*, **50**, 367 (1998).
Praveen, T., *Drug Delivery Devices*, Marcel Dekker, New York (1988).
Probstein, R. F., *Physiochemical Hydrodynamics*, Butterworths, Boston, pp. 41–45 (1989).
Rodrigues, A. E., J. M. Loureiro, C. Chenou, and M. Rendueles de la Vega, "Bioseparations with Permeable Particles," *J. Chromatog. B.*, **664**, 233 (1995).
Sassi, A. P., H. W. Blanch, and J. M. Prausnitz, "Phase Equilibria for Aqueous Protein/Polyelectrolyte Gel Systems," *AIChE J*., **42**, 2335 (1996).
Tong, J., and J. L. Anderson, "Partitioning and Diffusion of Proteins and Linear Polymers in Polyacrylamide Gels," *Biophys. J.*, **70**, 1505 (1996).
Tyn, M. T., and T. W. Gusek, "Prediction of Diffusion Coefficients of Proteins," *Bioeng. Biotechnol.*, **35**, 327 (1990).
Weaver, L. E., and G. Carta, "Protein Adsorption on Cation Exchangers: Comparison of Macroporous and Gel-Composite Media," *Biotechnol. Prog.*, **12**, 342 (1996).
Wright, P. R., F. J. Muzzio, and B. J. Glasser, "Batch Uptake of Lysozyme: Effect of Solution Viscosity and Mass Transfer on Adsorption," *Biotechnol. Prog.*, **14**, 913 (1998).
Yoshida, H., M. Yoshikawa, and T. Kataoka, "Parallel Transport of BSA by Surface and Pore Diffusion in Strongly Basic Chitosan," *AIChE J.*, **40**, 2034 (1994).

Manuscript received Sept. 2, 2002, and revision received Dec. 17, 2002.